DESIGN AND SUSTAINABILITY OF A PRESTRESSED AND PRECAST PEDESTRIAN BRIDGE MADE OF TEXTILE-REINFORCED CONCRETE

Christian Kulas, Institute of Structural Concrete, RWTH Aachen University, Germany
Josef Hegger, Institute of Structural Concrete, RWTH Aachen University, Germany
Claus Goralski, H+P Ingenieure GmbH & Co. KG, Aachen, Germany
Roland Karle, Groz-Beckert KG, Albstadt, Germany

ABSTRACT

Textile-reinforced concrete (TRC) is an innovative composite material which uses mesh-like textile reinforcements and a fine-grained concrete as basic materials. Unlike steel, textiles are not susceptible to corrosion, thus it is possible to minimize the concrete cover to only a few millimeters. As a result, slender concrete constructions can be built, meeting the needs of modern architecture with both economical and environmental advantages.

This paper presents a pedestrian bridge with a superstructure made of TRC which has a total length of 318 ft (97 m). It focuses on details of the design, construction, and dynamic behavior of the TRC bridge. Furthermore, beneficial aspects of sustainability are demonstrated from minimizing the cross-section, thereby saving concrete, and reducing carbon dioxide emissions in the production process, compared to ordinary steel-reinforced bridges. Finally, TRC construction results in environmental advantages mainly due to lower maintenance costs and, thus, lower life-time costs.

Keywords: TRC, slender, light-weight, sustainability, economic, environmental

INTRODUCTION

Textile-reinforced concrete (TRC) is an innovative composite material which uses mesh-like reinforcements made of alkali-resistant glass (AR-glass) or carbon. In contrast to ordinary steel reinforcements, the textile reinforcements do not corrode and, thus, the concrete covers can be minimized, leading to extremely thin and slender concrete constructions. Due to the small openings of the textile meshes, a fine-grained concrete with maximum grain sizes of about 0.20 in (5 mm) is necessary to allow for an unproblematic casting and penetration of the concrete through the meshes.

Today, textile-reinforced concrete is often used as construction material for façade structures. By using concrete covers of about 0.4 in to 0.6 in (10 mm to 15 mm) it is possible to reduce the weight of the structure by over 50%, compared to ordinary steel reinforced constructions. HEGGER et al. and KULAS et al. give detailed information on applications with TRC, especially ventilated façade structures, sandwich panels[1,2,3], as well as the load-bearing behavior of textile reinforcements[4]. Another field of application is in the construction impact from chlorides, e.g. due to de-icing salt. One example can be seen in a pedestrian bridge made of TRC described in detail within the scope of this paper.

Existing bridges made of steel-reinforced concrete often show damages induced by the corrosion of the reinforcement. The concrete covers of those constructions were designed in accordance to former standards, but are too small with regard to the required corrosion protection of steel reinforcement against carbonation and chloride ingress, leading to cracking and spalling of the concrete. These damages cause optical detractions on one hand, and on the other a reduced load-bearing capacity of the construction. The consequence is that these structures have to be improved by cost-intensive actions or replaced entirely by new structures. One example of an older bridge damaged by corrosion of the reinforcement is the pedestrian bridge over a state road in Albstadt, Germany. Due to immense corrosion damages, this bridge had to be torn down and replaced by a new bridge, Fig. 1.

Fig. 1 Pedestrian Bridge with TRC superstructure in Albstadt, Germany

Fulfilling demands on a frost-resistant construction, the superstructure of the new bridge is made of TRC, since the textiles are resistant against the impact of chlorides, e.g. de-icing salt. Furthermore, the concrete cover can be minimized to only a few millimeters, resulting in a slender, light-weight, and sharp-edged construction with a high-quality and fair-faced concrete surface. Regarding the bridge in Albstadt, concrete covers of 0.6 in (15 mm) are realized.

This paper gives detailed information on the design of the world's largest TRC construction. The results of the structural analysis, especially the dynamic behavior and the experimental investigations, are presented. In addition, the article focuses on certain sustainability aspects from the use of TRC: Contrary to constructions made of standard concrete, the TRC superstructure can be realized without any bitumen surfacing due to the denser nature of fine-grained concrete. As a result, maintenance work can be minimized, allowing for a more economical construction, since surfaces made of bitumen typically need to be renewed several times within the lifetime of the bridge. Finally, due to high savings of concrete, TRC constructions enable significant CO_2 emission reductions compared to steel-reinforced constructions allowing for a greener construction.

MATERIALS

TEXTILE REINFORCEMENT

TRC uses mesh-like non-corrosive reinforcements usually made of filaments with AR-glass or carbon as basic materials. GRIES et al. gives general information on properties and fabrication of textiles[5]. Carbon is advantageous in its high tensile strength (over 2,000 MPa), but was lacking in availability in the planning phase of the bridge and is comparatively more expensive than AR-glass. Thus, AR-glass filaments are used in the pedestrian bridge, where hundreds of filaments are bundled into each roving as depicted in Fig. 2a.

a) 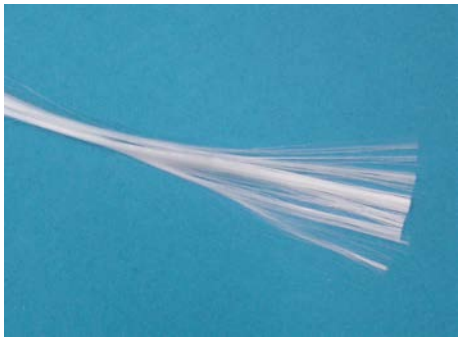 b) 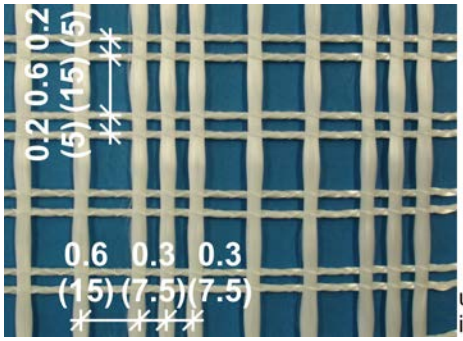

Fig. 2 a) Roving made of AR-glass filaments; b) Laid-Scrim

The rovings are finished into a laid-scrim with distances between 0.2 in and 0.6 in (5 mm and 15 mm), Fig. 2b. In the next production step, the laid-scrim is impregnated with epoxy resin. RAUPACH et al. refers to the advantages of impregnated textiles in comparison to those which are not impregnated[6]. Since the filaments have diameters of

only a few micrometer the concrete matrix cannot penetrate into the inner rovings due to the small space between the single filaments and, thus, the core filaments are not activated for load transfer. By impregnating the textiles with, for example, epoxy resin the resin can penetrate deep into the roving and connect the filaments with each other, creating a homogenous cross-section where nearly all filaments are activated for load transfer. As a result, the tensile strength can be more than doubled in comparison to non-impregnated rovings.

After applying the resin, the textiles have to be cured under high temperatures. Here, two different procedures can be distinguished: curing immediately after the coating process or first coating with a thermoset resin and curing sometime later. In the first procedure, the textile is driven through a tray filled with fluid epoxy resin. Immediately after this process, the wet mesh runs up into a drying tower operated at temperatures of about 320°F (160°C) where the resin is hardened, resulting in a planar reinforcement structure. The second procedure is necessary to produce spatial reinforcement structures, e.g. reinforcement for concrete webs. The resin remains in what is known as a "B-stage", where it is not hardened yet and continued processing is still possible. After laying the mesh into a mold of any shape and compressing it, the mold is placed in an oven and cured at a temperature of 356°F (180°C) for 20 min[7].

Impregnated textile structures are inherently stable and have a good handling as well as workability. This is necessary for using them for large-scale members under practical conditions in precast concrete factories. Furthermore, by impregnation with epoxy resin the durability of AR-glass textiles can be greatly enhanced[8]. The main properties of the textile used in this project are specified in Table 1.

Table 1: Main properties of the textile reinforcement

Property		Unit	Value
Roving	Producer	-	OCV™ Reinforcements
	Denotation	-	LTR 5325
	Titer	tex[1)]	3,600 (= 1,200+2,400)
	Elastic modulus	MPa	64,800
Impregnation	Producer	-	Epoxy resin (Momentive Specialty Chemicals Inc.[2)])
Roving distances	0° / 90°	in	0.2 ; 0.6 / 0.3 ; 0.6
		mm	5 ; 15 / 7.5 ; 15
Cross-Section	0° / 90°	in^2/ft	0.063 / 0.056
		mm^2/m	134 / 119
Tensile strength[3)]	0° / 90°	MPa	1,035 / 1,194

1) 1 tex = 4.3×10^{-5} lb/ft = 1000 g/km
2) formerly: Hexion Specialty Chemicals, Inc.
3) Tensile strength of the textile reinforcement determined in concrete (mean values)

FINE-GRAINED CONCRETE

Since the openings between the rovings are relatively small, a concrete with a small grain size has to be used to ensure a proper penetration of the textiles in the concrete. The fine-grained concrete was developed at the Collaborative Research Center 532 (SFB 532) at RWTH Aachen University[9]. Since this laboratory concrete mixture of the SFB 532 has a maximum grain size of 0.024 in (0.6 mm), in this project a concrete matrix with an enlarged maximum grain-size of 0.16 in (4.0 mm) is used. A larger grain size comes along with a smaller cement amount and, thus, the workability can be enhanced. This matrix was developed in cooperation between the construction company Sebastian Wochner GmbH & Co. KG and the Institute of Building Materials Research at RWTH Aachen University. The main properties of this high performance concrete are specified in Table 2.

Table 2: Main properties of the fine-grained concrete

Property	Unit	Value
Maximum grain-size	in	0.16
	mm	4
Strength class	-	C55/67
Compressive strength	MPa	87.1
Flexural strength	MPa	10.7

DESIGN PARAMETER

The pedestrian bridge has a total length of 318 ft (97 m) and is subdivided into six parts, where each part of the superstructure is a precast TRC element. The maximum length of those elements is 56 ft (17.20 m), while the maximum span is 49 ft (15.05 m). The cross-section of the superstructure is a 11 ft (3,210 mm) wide concrete T-beam with seven webs, each prestressed by four single-strand cables (unbounded prestressing) and reinforced with three GFRP-bars in addition to the textile reinforcement, Fig. 3.

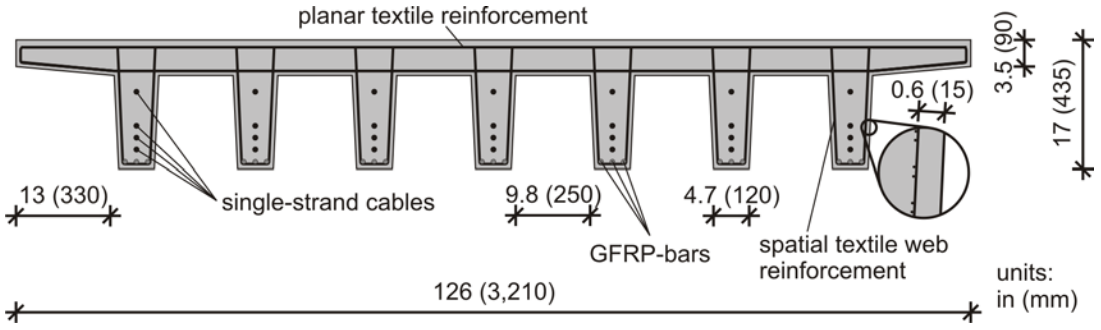

Fig. 3 Cross-section of the TRC superstructure

The textile reinforcement of the webs is made of U-shaped textiles, which intersect the lower layer of the planar reinforcement of the slab. These U-shaped textiles are anchored in the slab and reached up to the upper slab reinforcement. While the bending moment is borne by textiles, GFRP-bars and single-strand cables, the shear reinforcement in the webs consists only of textiles.

The concrete cover of 0.6 in (15 mm) is determined by considering the maximum grain size and geometrical tolerances during the concreting process while ensuring a sufficient bond between the textile and concrete. The concrete cover and small bending diameter of the textiles (approximately 0.3 in (8 mm)) affords a minimum thickness of the bridge deck of only 3.5 in (90 mm) at the end of the two cantilever sections and 4.7 in (120 mm) as the minimum web thickness. The slab thickness is also 4.7 in (120 mm), where the upper 0.4 in (10 mm) is used as an abrasion layer to resist the mechanical action of pedestrians, bicycles, and snow ploughs during winter times. No further covering of the walkway is necessary. With a height of the superstructure of only 17.1 in (435 mm) the whole construction has an extremely small slenderness ratio of H:L = 1:35.

The construction has to resist the following actions, specified in the structural analysis and verified within a large-scale testing program:

Ultimate limit state (ULS):	- dead loads
	- live loads due to pedestrian and wind
	- snow ploughs (max. weight 5.5 ton)
Serviceability limit state (SLS):	- decompression (“frequent combination“)
	- crack width $w \leq 0.012$ in (0.3 mm) (“rare combination“)
Earthquake verification:	- earthquake zone 3 (a = 2.6 ft/s^2 (0.8 m/s^2))
Oscillation verification:	- limit of the vertical acceleration $a_v \leq$ 2.3 ft/s^2 (0.7 m/s^2)
	- limit of the horizontal acceleration $a_h \leq$ 0.7 ft/s^2 (0.2 m/s^2)

STRUCTURAL ANALYSIS

CROSS-SECTION CAPACITY

The internal forces, concrete stresses and forces of the post-tensioning system are determined with a three-dimensional finite-elements model, Fig. 4.

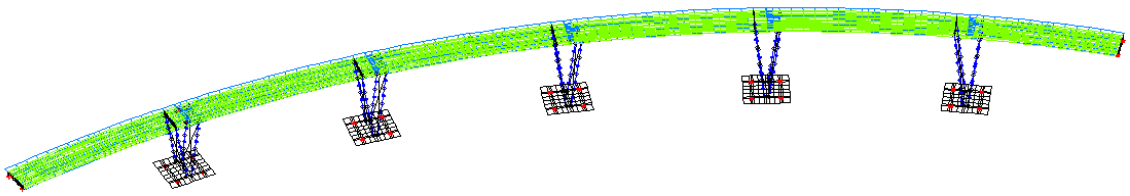

Fig. 4 Finite-elements model of the whole bridge

Within the model the superstructure is generated with shell-elements and the columns with beam-elements. Furthermore, due to the high exploitation of the cross-section this model is also used to assess the oscillation behavior.

Considering the internal forces of the slab, the required textile reinforcement is defined. In order to increase the robustness of the member, all of the webs are fully prestressed with four single-strand cables, Fig. 3. The internal forces (*M*, *N*, *V*) of the individual webs could be calculated by stress-integration, Fig. 5.

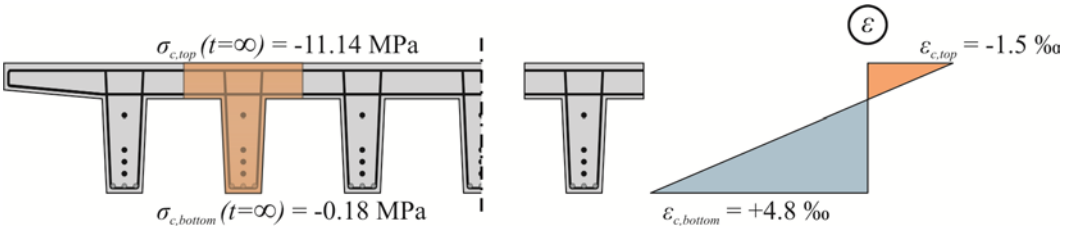

Fig. 5 Decompression and strain distribution in ULS

Since the footprint of the bridge is a circular one, the TRC-elements of the superstructure are produced with a radius of about 367 ft (112 m). With a growing radius from the inner part of the circle to the outer part, the moment-load of the webs increases. An increased lever arm of the single-strand cables counters the growth of the bending moment from the inner to the outer web.

OSCILLATION BEHAVIOR

Currently introduced standards do not contain a complete concept for the verification of the oscillation behavior for pedestrian bridges. Since pedestrian bridges are able to oscillate due to pedestrians or cyclist, coordination with the client is necessary. According to the German standard “DIN Fachbericht 102”, natural frequencies between 1.6 Hz and 2.4 Hz are recommended for concrete bridges[10], and structures with low rigidity and absorbability, the interval between 3.5 and 4.5 Hz should be avoided. However, for slender structures like the bridge in Albstadt, these limits cannot be adhered to. Therefore more detailed calculations are required in order to open up new dimensions of slenderness for modern architecture and simultaneously guarantee the safety against objectionable oscillation. The rating of oscillation-sensitivity by CHARLES and HOORPAH on the basis of natural frequencies also highlights this[11]. In Table 3 the range of the eigenmode values are shown.

Table 3: Rating of the oscillation sensitivity[11]

risk of resonance	eigenmode [Hz]	
	vertical	lateral
high	$1.7 < f_v \leq 2.1$	$0.5 < f_l \leq 1.1$
low	$2.6 < f_v \leq 5.0$	$1.3 < f_l \leq 2.5$

$f_{1,longitudinal}$ = 1.6 Hz

$f_{5\text{-}6,vertical}$ = 3.1 Hz

$f_{2\text{-}4,transversal}$ = 1.6 Hz

The calculation of the complete system always shows superposed eigenmode. It contains the vertical and horizontal eigenmodes of the superstructure as well as the eigenmode of the columns and the bracing, Fig. 6.

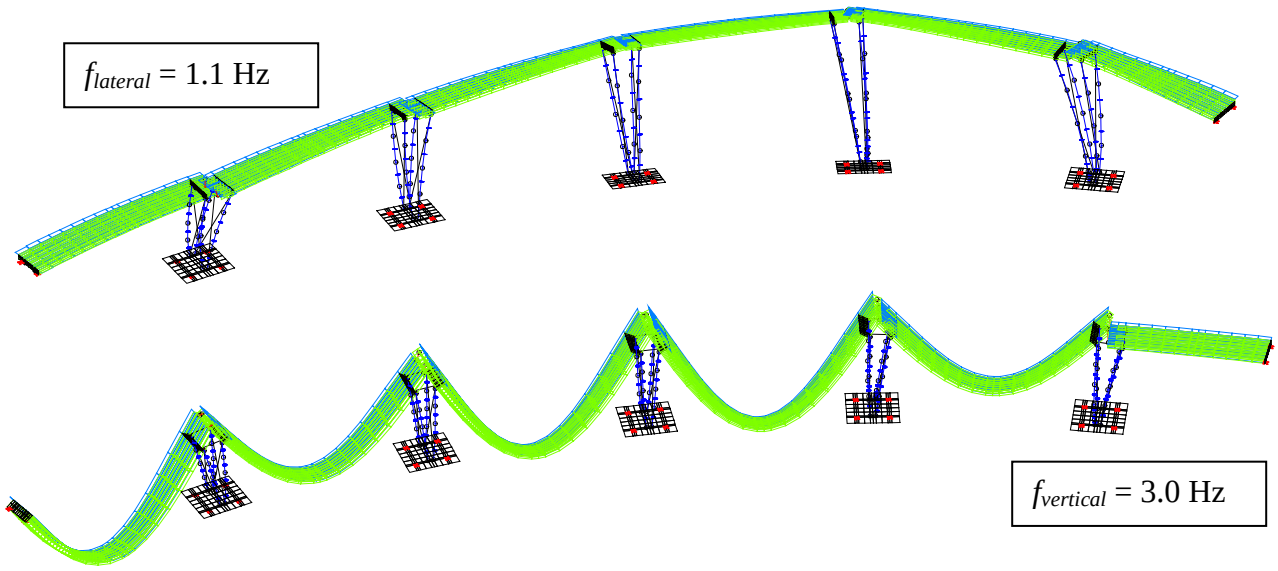

Fig. 6 Characteristic eigenmode calculated by the finite-element model

CHARLES and HOORPAH carried out a rating of the calculative acceleration[11]. For the pedestrian bridge in Albstadt, the vertical ($a_{vert,1}$) and horizontal ($a_{lat,1}$) acceleration for a jogger running in resonance, a group of people (n = 13 persons), and a stream of people (n = 0.056 person/ft^2 × bridge-area (0.6 person/m² × bridge-area)) are calculated. The coefficients k_{vert} and k_{hor} are used to consider the probability of step-frequencies in reference to the natural frequencies calculated manually, Fig. 7.

The calculative accelerations are:

Pedestrians:
$a_v = 0.82$ ft/s^2 < 2.30 ft/s^2
($a_v = 0.25$ m/s^2 < 0.7 m/s^2)
$a_h = 0.03$ ft/s^2 < 0.66 ft/s^2
($a_h = 0.01$ m/s^2 < 0.2 m/s^2)

A Group of people:
$a_v = 1.80$ ft/s^2 < 2.30 ft/s^2
($a_v = 0.55$ m/s^2 < 0.7 m/s^2)
$a_h = 0.07$ ft/s^2 < 0.66 ft/s^2
($a_h = 0.02$ m/s^2 < 0.2 m/s^2)

A Stream of people: $a_v = 2.76$ ft/s^2 ~ 2.30 ft/s^2
($a_v = 0.84$ m/s^2 ~ 0.7 m/s^2)
$a_h = 0.62$ ft/s^2 < 0.66 ft/s^2
($a_h = 0.19$ m/s^2 < 0.2 m/s^2)
Jogger: $a_v = 4.76$ ft/s^2 > 2.30 ft/s^2
($a_v = 1.45$ m/s^2 > 0.7 m/s^2)

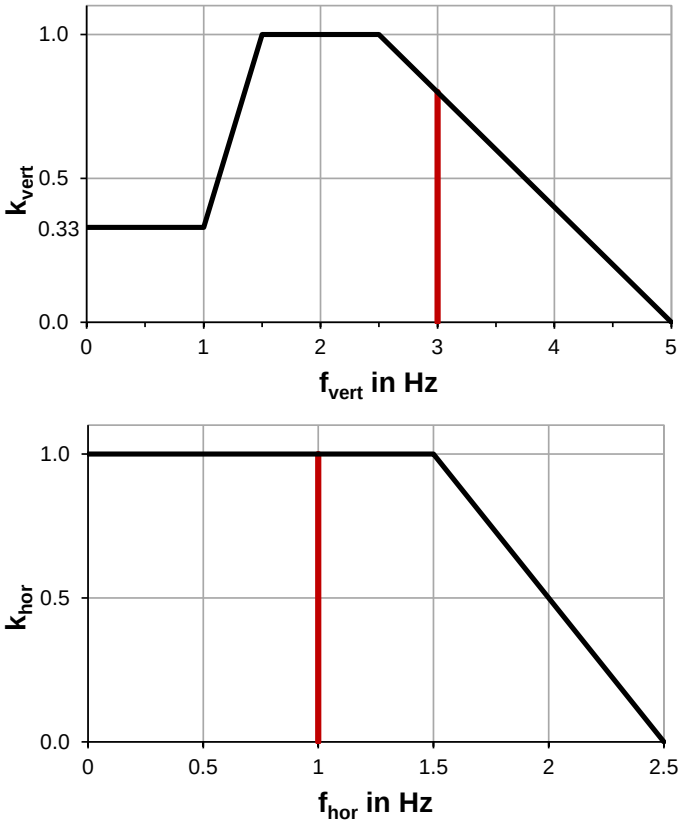

Fig. 7 Step-frequencies in reference to natural frequencies

The results are evaluated as follows:

- The horizontal acceleration longitudinal to the bridge (1. eigenmode) can be classified as uncritical as it is very difficult for a pedestrian to initiate it.
- The verification of the vertical and lateral acceleration for pedestrians and a group of people (n = 13 persons) is achieved.
- The vertical acceleration due to a stream of people is within the range of the border-accelerations of the "DIN Fachbericht 102"[10] ($a_{max} < 0.5 x f_0^{0.5} = 2.89$ ft/s^2 (0.88 m/s^2)), but outside the comfortable range of $a < 2.30$ ft/s^2 (0.7 m/s^2)
- The acceleration due to a jogger exceeds the maximum vertical acceleration of 2.30 ft/s^2 (0.7 m/s^2) clearly. This cannot be noticed by a jogger or a pedestrian. All in all, this can be classified as uncritical.
- The verification of the lateral acceleration caused by a stream of people kept within range. The influence of synchronization of the pedestrians (lock-in effect) was tested within a field test and was classified as uncritical.

EXPERIMENTAL INVESTIGATION

Since textile-reinforced concrete is not regulated by any standards in Germany today, an individual approval of the construction by the building authorities is required. Therefore a large-scale testing program was conducted. Within the scope of this paper, the load-bearing behavior of the slab and the longitudinal beam under shear force are presented, describing the main tests in transverse and longitudinal direction of the bridge, as well as showing the results of a full-scale bending test.

LOAD-BEARING BEHAVIOR OF THE BRIDGE SLAB

The load-bearing behavior of the slab was determined with standard four-point bending tests on specimens matching the real dimensions of the bridge-slab. While the bridge deck will have a slab thickness of 4.72 in (120 mm) at the beginning, the slab thickness of the specimens was set to 4.33 in (110 mm) in order to include the effect of abrasion, which was estimated to be 0.4 in (10 mm) at the end of the bridge lifetime. The load-bearing behavior of the cantilever of the bridge under bending moments is assessed with the test setup shown in Fig. 8.

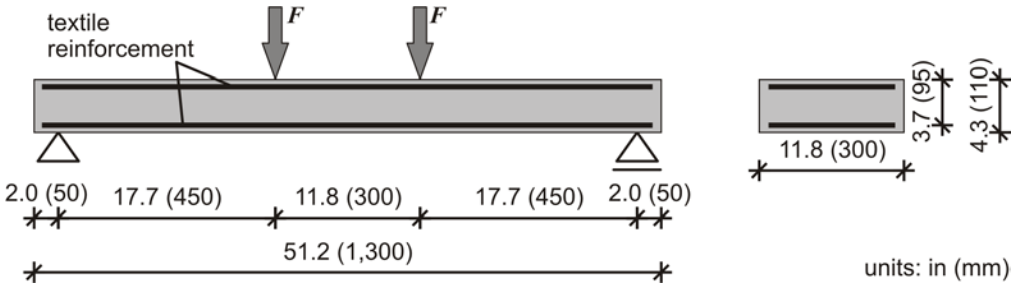

Fig. 8 Setup of slab-tests

Due to the high reinforcement area in the slab, all specimen failed by reaching the maximum shear force. Fig. 9 depicts the ultimate limit state (ULS), where a diagonal tension failure is shown as the primary failure. As second failure, a horizontal crack on the level of the reinforcement is recognized. Both the primary and the secondary failures are typical for slabs without shear reinforcement and have been investigated on slabs with steel reinforcement as well. All tests show a distinctive crack pattern with small crack widths and distances, which is typical for TRC members.

Fig. 9 Failure mode of the slab-test

Fig. 10 shows the textile tensile stress over the deflection. Compared to the values of the textile strength in Table 1, which are determined in a tensile test, the values in the bending tests are about 45% higher, reaching a mean value of about 1500 MPa. HEGGER and VOSS explain this effect with an activation of the filaments in the inner core of the roving due to the deflection of the rovings at the edge of a crack[12]. Since the rovings used in this project are impregnated it is questionable if this effect is decisive here, even under the assumption that rovings are not perfectly impregnated; rather an increased bond between roving and concrete could instead be the cause of the higher tensile values. Current studies are further investigating this effect.

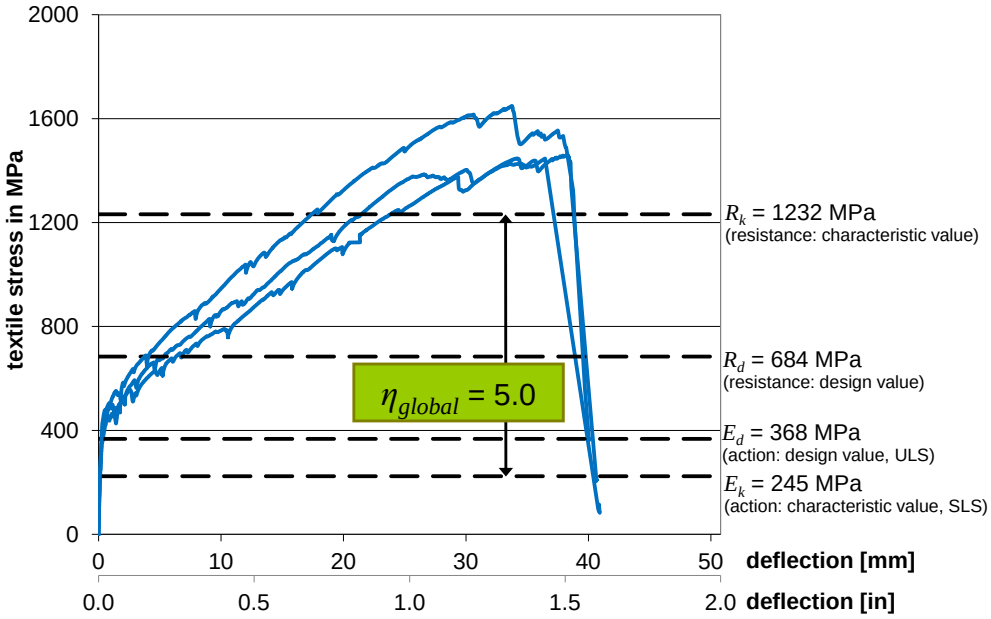

Fig. 10 Slab-tests: textile stress – deflection diagram

In the serviceability limit state (SLS) the client requires a maximum crack width of 0.012 in (0.3 mm). This criterion was fulfilled since in SLS all specimens remained uncracked. Furthermore, the margin between the characteristic value of the resistance R_k and action E_k indicates a high global safety factor η_{global} = 5.0.

LOAD-BEARING BEHAVIOR OF THE T-BEAM

With the test setup depicted in Fig. 11, the load-bearing behavior of the bridge in longitudinal direction under shear forces is investigated. Due to limitations from the width of the testing machine, the specimens were tested with three instead of seven webs, extrapolating the test results to seven webs. By applying the point load at a distance of 47 in (1.20 m) apart from the support, the ratio of the distance from the support over the effective depth is a/d = 3.15, thus, ensuring the determination of the minimum shear resistance of the beam. In addition, the point load is applied eccentrically to consider minor torsional effects.

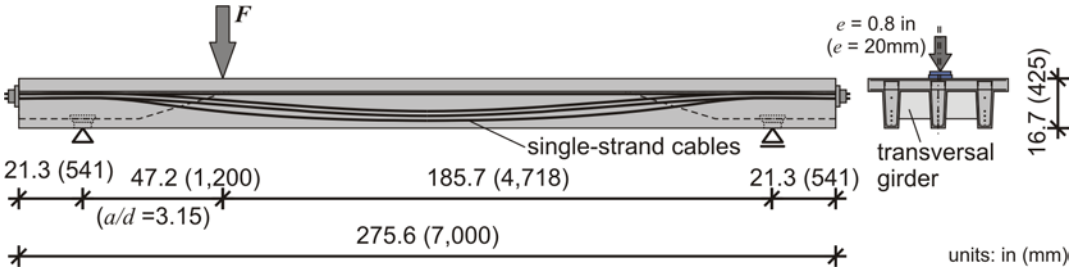

Fig. 11 Test setup of the longitudinal beam

The state of failure is characterized by collapsing of the compression zone, while in SLS the members remained uncracked. On the horizontal axis of the diagram in Fig. 12, the deflection related to the span of the specimens is shown. Here, the members achieve high deformations in ULS in the range of 1/200 to 1/150 of the span. High deformations and a stabilized crack pattern (Fig. 13) signalize the collapsing of the member, thus, no sudden failure was observed. Overall, a global safety factor η_{global} = 5.0 was achieved here as well.

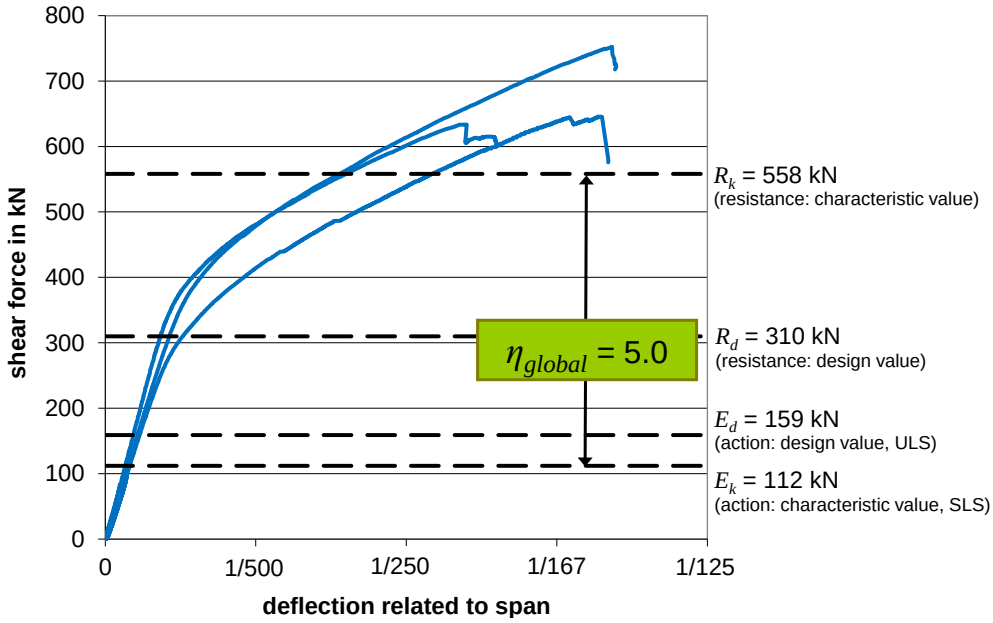

Fig. 12 Longitudinal beam: maximum shear force

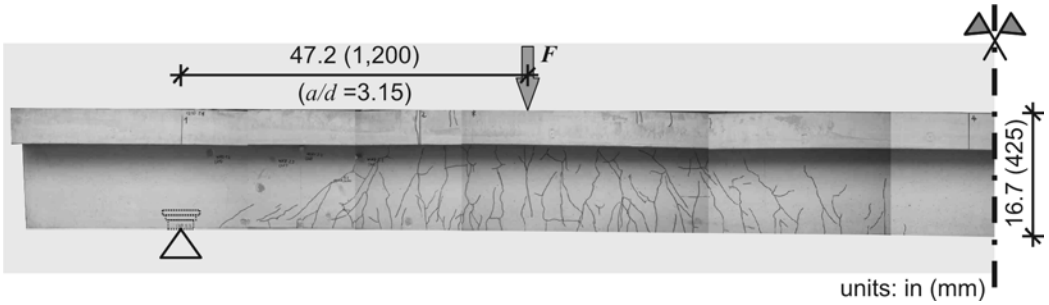

Fig. 13 View of the longitudinal beam with crack pattern in ultimate limit state

FULL-SCALE BENDING TEST

In addition to the 23.0 ft (7.0 m) long specimens the bending-behavior was also tested within a full-scale test on a real bridge element. With realistic dimensions of a length of 56.4 ft (17.20 m), a width of 10.5 ft (3.21 m) and a span of 49.4 ft (15.05 m), the specimen was tested on the building yard of the construction company. The element was erected on concrete supportings, which had a height of 2.0 ft (0.6 m). The load was brought up successively by concrete blocks arranged in the middle of the element on an area of about 6.6 ft × 10.5 ft (2.0 m x 3.21 m), Fig. 14.

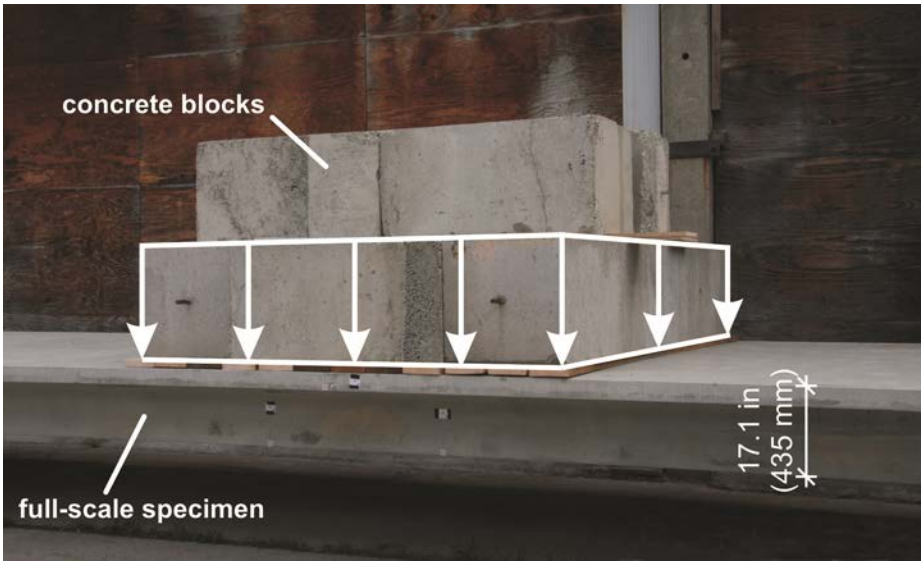

Fig. 14 Load-application within the full-scale test

On the load level, where according to the structural analysis first cracks should appear, the specimen still remained uncracked. Only until a load of roughly 83 tons (about 80% of the maximum load), corresponding to a bending moment of 2.065×10^6 ft-lb (2,800 kNm), did the crack width reach 0.012 in (0.3 mm). This is the maximum crack width allowed by the bridge owner, occuring at a load level over two times the calculated value for first cracks to occur (0.885×10^6 ft-lb (1,200 kNm)).

The maximum load applied on the specimen, was about 103 tons, Fig. 15a. The test was stopped at this load level, only because the applied concrete blocks reached a critical height at which it became dangerous for the staff around the specimen. At the maximum applied load, the deflection was defined and evident, reaching about 20 in (0.5 m), Fig. 15b, with the maximum crack width measuring 0.024 in (0.6 mm).

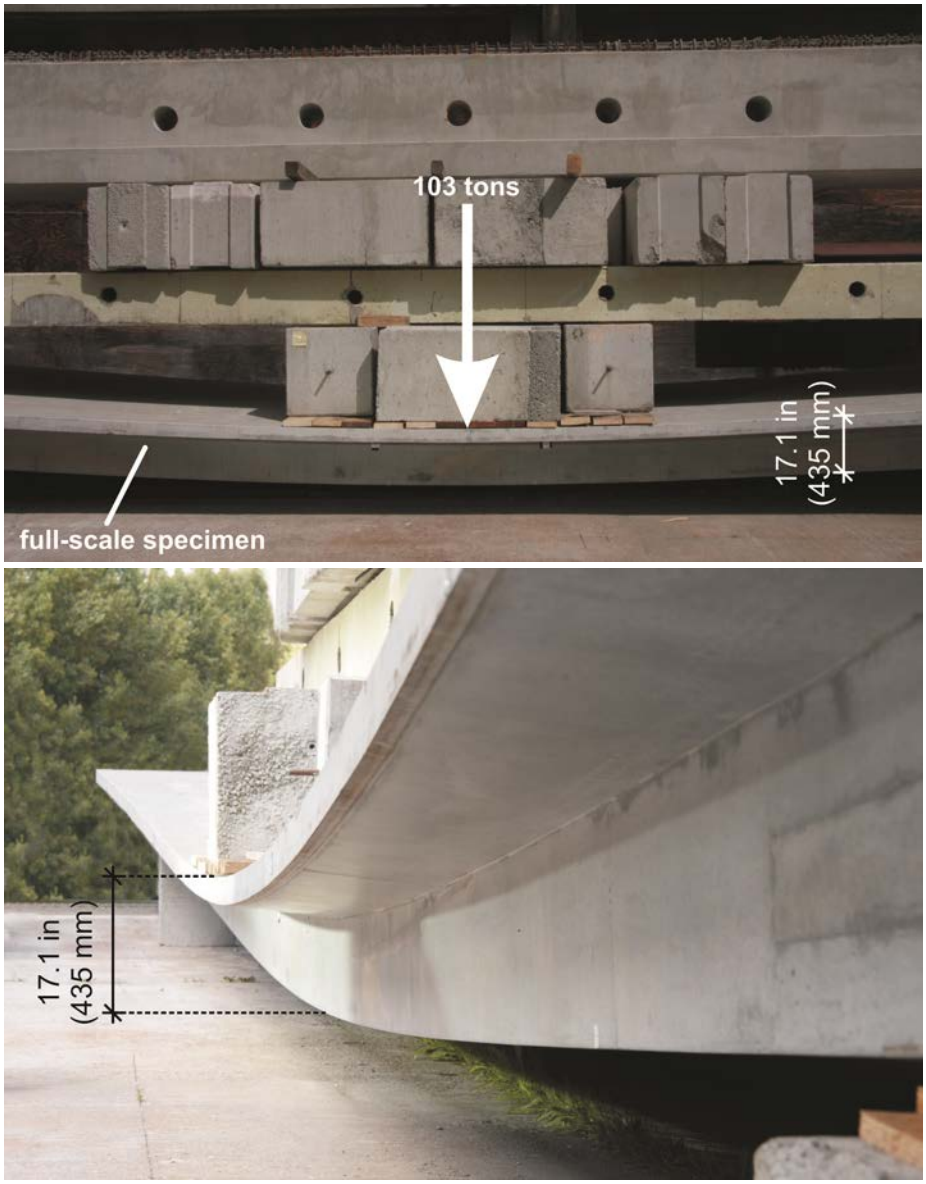

Fig. 15 Deflection under maximum load: a) front view; b) view in longitudinal direction

SUSTAINABILITY

ASSUMPTIONS FOR CALCULATION

For the analysis of the lifetime costs and carbon dioxide (CO_2) emissions, the TRC cross-section is compared with an ordinary bridge construction made of steel-reinforced concrete (SRC), following the specifications of the German guideline ZTV-ING[13]. Like the TRC construction, the SRC cross-section is also a T-beam, but instead of seven webs, only three webs with a larger thickness of 11.8 in (300 mm) are arranged, Fig. 16. The widths of both superstructures are the same, but due to larger concrete cover and bending diameters of the steel bars, the SRC solution has a total height of 25.2 in (640 mm). Furthermore, a 7.9 in (200 mm) thick slab is used instead of 4.7 in (120 mm) for the TRC

construction. In contrast to the TRC bridge, which was designed without further surfacing layers, the SRC bridge design included an additional layer of melted asphalt[13].

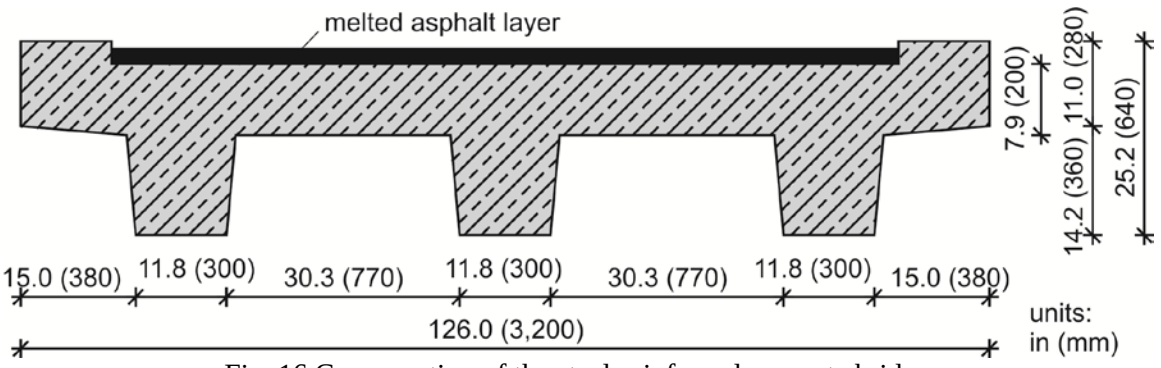

Fig. 16 Cross-section of the steel-reinforced concrete bridge

The material costs are the basis for the analysis of the costs and are summarized in Table 4. For calculating the labor costs, a wage per hour of $45 was assumed and 300 $/ton is assumed for the cost of steel reinforcements, including labor and installation costs. Within the calculation the foundation for both variants is assumed to be the same. Further optimization and, therefore, costs and materials reduction are possible.

Table 4: Material costs

		Unit	Value	Unit	Value
a) TRC					
Fine-grained concrete C55/67		$/ft^3	4.5	$/m³	160
Planar textile reinforcement		$/ft²	1.9	$/m²	20
Shaped textile reinforcement		$/element[1)]	30	$/element[1)]	30
Single strand cables 1600/1860		$/ft	6.1	$/m	20
GFRP bars Ø0.6 in (Ø16 mm)		$/ft	3.0	$/m	10
b) SRC					
Standard concrete C55/67		$/ft³	2.8	$/m³	100
Steel bars	Ø0.3 in (Ø8 mm)	$/ton	1,016	$/tonne	1,120
	Ø0.4 in (Ø10 mm)	$/ton	962	$/tonne	1,060
	Ø0.8 in (Ø20 mm)	$/ton	835	$/tonne	920
Forming stirrups		$/stirrup	0,40	$/stirrup	0,40
Single strand cables 1600/1860		$/ft	6.1	$/m	20
Melted asphalt		$/ton	82	$/tonne	90

[1)] element length = 6.6 ft (2.0 m)

ECONOMICAL ANALYSIS

Based on the cross-sections depicted in Fig. 3 and Fig. 16, the masses for a 56.4 ft (17.20 m) long bridge element were determined. The results are shown in Fig. 17 for the main structural elements.

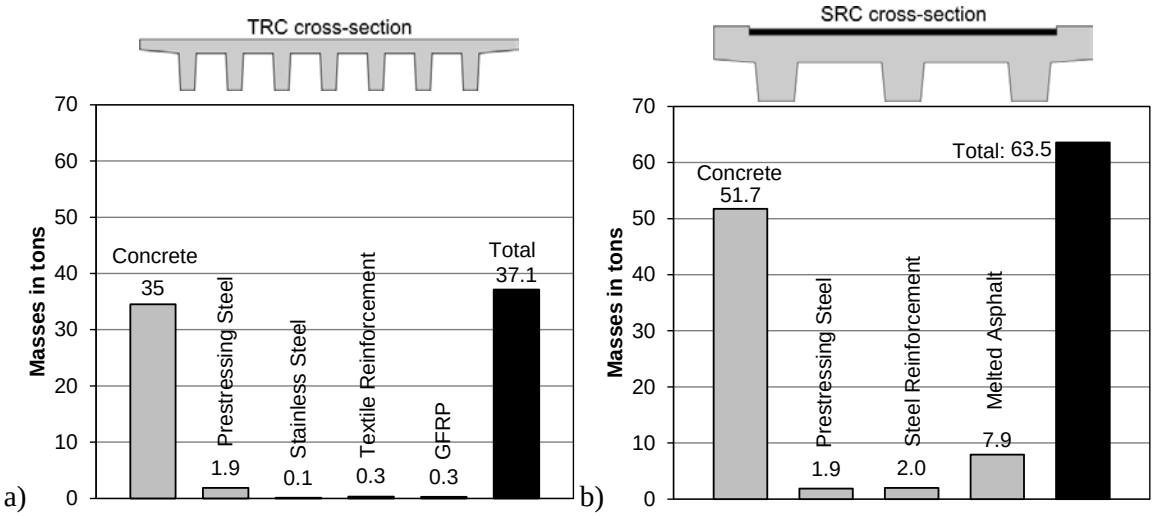

Fig. 17 Masses of the main constructional elements: a) TRC; b) SRC

The TRC element has a total mass of about 37 ton, which is 58% of the mass of the SRC construction. To make a precise calculation of the total costs, it is necessary to consider the shape of the bridge's footprint. The pedestrian bridge in Albstadt has a circular footprint with a radius of about 367 ft (112 m), however, the calculation is based on a straight footprint with linear elements for both the TRC and the SRC construction. It is assumed that due to the curvature of the footprint the costs of the formwork and installation of the textile reinforcement are 40% higher than the straight solution. From the assumptions made in the previous section and the calculated masses in Fig. 17, the costs for both bridge constructions can be determined and are depicted in Fig. 18.

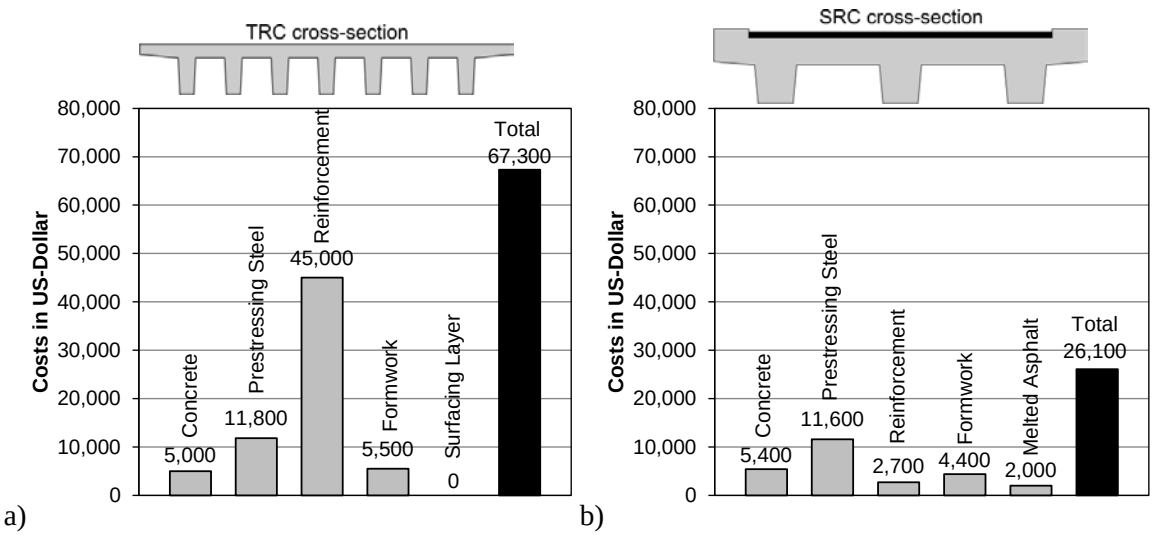

Fig. 18 Costs of the main constructional elements: a) TRC, b) SRC

The results show that the overall cost of the textile reinforced construction is approximately 2.5 times higher than that of the steel-reinforced variant, and the influence of the concrete savings on the overall costs is relatively small. While the TRC solution reduces the mass of the concrete by about 30%, the material costs are actually higher compared with typical concrete, since the fine-grained concrete consists of a large amount of cement, thereby offsetting the advantage of the lower mass.

Nearly 70% of the total costs for TRC are due to the production, preparation and installation of the textile reinforcement. The detailed costs broken down for each production step are depicted in Fig. 19a. Much of the costs comes from cutting and installing the reinforcement. Since the vertical stirrups of the web reinforcement intersect the lower layer of the slab reinforcement, the interfering longitudinal rovings have to be cut out, Fig. 19b. This work can only be manually done with the help of a circular saw, however, this is extremely time- and cost-intensive. Currently, an active industrial research project is focusing on the optimization of this task and considering automatic or semi-automatic solutions.

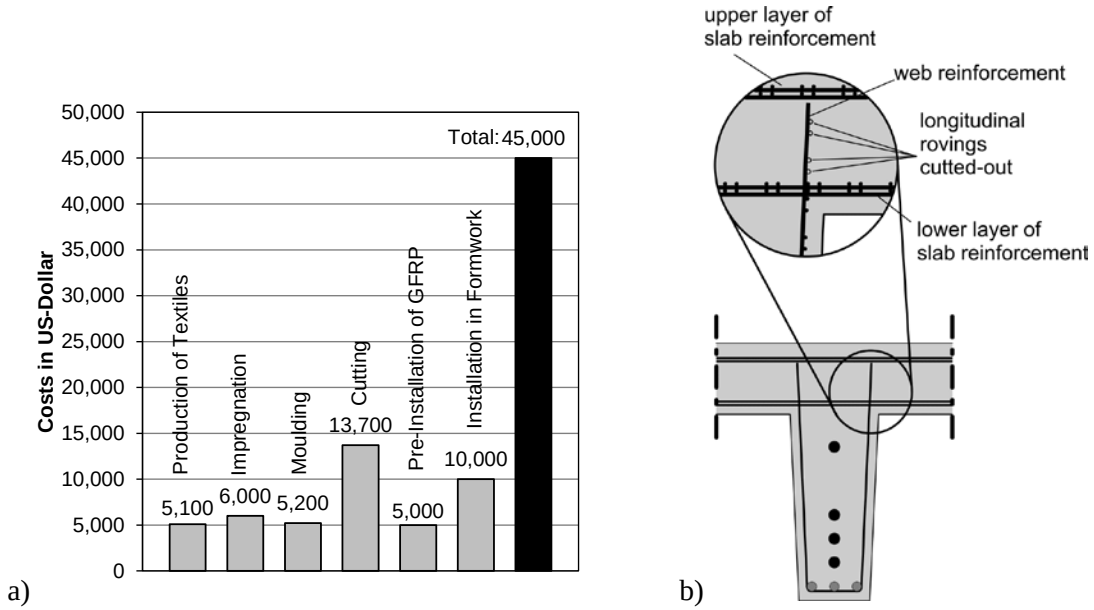

Fig. 19 a) Costs of producing and installing the textile reinforcement
b) Intersection of web and slab reinforcement

While the costs shown in Fig. 18 for the textile-reinforced bridge are realistic values for the prototype bridge in Albstadt, a steel-reinforced bridge can be produced on an industrial scale with lower costs as opposed to prototypes. As a result, serial production costs for both bridges have to be used for an accurate and proper comparison. The following assumptions have to be taken into account to estimate the costs for a serial production of a TRC bridge. First, in mass production, prototypical cutting and work costs can be reduced to zero, since interfering rovings can be left out initially during the production of the textiles. Furthermore, an industrial research project is currently working on an automated molding process for the production of shaped reinforcements. In addition, the workers in the factory did not have any experience in working with textile-

reinforced concrete. From installing the prestressed steel and textile reinforcement in the narrow parts of the formwork to concreting through the textile meshes, every production step can be optimized with increased experience in working with this composite material. Costs from an industrial production process are assumed to be 25% lower, resulting in production costs of: ($67,300 - $13,700)·0.75 = $40,200.

In order to assess the economic aspects of the construction, it is important to look not only on the production costs, but also on the lifetime costs, of 80 years in this case. The maintenance fees of a steel-reinforced bridge construction are approximately 4.0% of the production costs per year[14]. Those costs cover, for example, renewing the melted asphalt layer or substituting the supportings. Since the TRC bridge does not have a separate melted asphalt layer, the maintenance fee can be set much lower and is assumed to be 0.5% of the production cost per year. At the end of the lifetime, the cost for one bridge element is as follows:

TRC:	$40,200 + 80 years × 0.5% × $40,200	= $56,300
SRC:	$26,100 + 80 years × 4.0% × $26,100	= $109,600

Ultimately, the lifetime costs of the TRC bridge is about 50% cheaper in comparison with a steel reinforced construction, due to lower maintenance costs.

ENVIRONMENTAL ANALYSIS

Within the scope of this article, the environmental analysis focuses on the emission of carbon dioxide (CO_2), which is emitted in the production process of the main construction parts of the bridge. The CO_2 emissions are calculated with the program GEMIS (Global Emission Model for Integrated Systems[15]), which considers emissions from not only production processes but also transportation. In Fig. 20, the Greenhouse Warming Potential (GWP) for the main production processes and transportation of the TRC bridge and SRC bridge are depicted. The GWP is the CO_2-equivalent of the amount of greenhouse gas emissions, which influences the greenhouse effect. It considers not only the emission of CO_2, but also the emissions of other greenhouse gases, which are converted into equivalent CO_2 emissions. Research calculations show that there is evidence the overall GWP of the textile-reinforced bridge is 25% less than the steel-reinforced variant, because the production of the reinforcing steel is 15% more energy intensive compared to the production of the textiles. In contrast to the economic analysis, here the reduction of the concrete is essential for an ecological construction. The 30% reduction of concrete mass results in also a 30% reduction of CO_2 emissions. Further GWP reductions are due to avoiding the surfacing layer on the walkway and lower transportation costs due to the reduced weight of the elements.

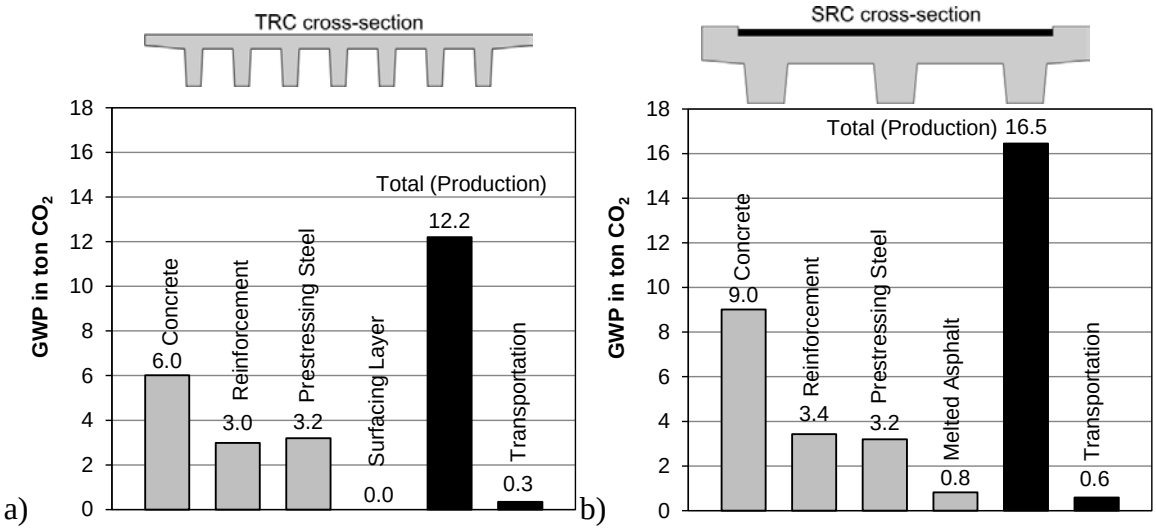

Fig. 20 Greenhouse Warming Potential (GWP) for the main production processes and transportation: a) TRC bridge; b) SRC bridge

CONCLUSIONS

In recent years, textile-reinforced concrete (TRC) has been often applied for small scale structural elements with simple load-bearing behavior and straightforward configurations of textile reinforcements. The example of the 318 ft (97 m) long pedestrian bridge with TRC superstructure in Albstadt, Germany, demonstrates that this innovative composite material can also be used for large-scale applications. Tests on the load-bearing behavior showed that next to the required safety-level, even further capacities are available. By comparing the cross-section of a TRC bridge with that of a steel-reinforced concrete bridge, it is shown that the TRC bridge offers economic and environmental advantages. Considering the lower maintenance work over the lifetime, the costs for a TRC construction are about 50% lower compared with a steel-reinforced bridge, and greenhouse gas emissions can be reduced by 25% using textile-reinforced concrete.

One 56.4 ft (17.20 m) bridge element is in fact installed on the company site of Groz-Beckert. In the winter, it is continuously loaded with a snow-removal vehicle and exposed with de-icing salt. The condition of this element is periodically observed and the deflections are continuously measured and compared to the allowable values.

The authors gratefully acknowledge the town of Albstadt, Germany, for their willingness to undertake this pilot project. The authors also thank Sebastian Wochner GmbH & Co. KG Dormettingen (construction company), H+P Ingenieure GmbH & Co. KG Aachen (structural analysis), the Regional Commission Tübingen (construction supervision) and hns architects Stuttgart (architectural design) for the efficient collaboration. The project was mainly financed by Groz-Beckert with the intention to show the capabilities of TRC. Groz-Beckert is heavily involved in the technical transfer of TRC from the university to the industry and is preparing a pre-production line for textile reinforcement.

REFERENCES

1. Hegger, J., Kulas, C., Horstmann, M., „Realization of TRC facades with impregnated AR-glass textiles", *Key Engineering Materials*, Vol. 466, 2011, pp. 121-30.
2. Kulas, C., Schneider, M., Will, N., Grebe, R., "Ventilated facade structures made of textile reinforced concrete - structural behavior and construction". *Bautechnik*, Vol. 88, Issue 5, 2011, pp. 271–280.
3. Hegger, J., Horstmann, M., Feldmann, M., Pyschny, D., Raupach, M., Büttner, T., Feger, C., "Sandwich Panels made of TRC and Discrete and Continuous Connectors", In: Brameshuber, W., *Proceedings of the 2nd International RILEM Conference on Material Science (MatSci)*, September 6-8, 2010, Aachen, Germany. RILEM Publications S.A.R.L., pp. 381-392.
4. Hegger, J., Will, N., Bruckermann, O., Voss, S., „Load-bearing behaviour and simulation of textile reinforced concrete", *Materials and Structures*, Vol. 39, Issue 8, 2004, pp. 765-776.
5. Gries, T., Roye, A., Offermann, P., Peled, A., "Textiles". In: Brameshuber, W. (Edt.), *Textile Reinforced Concrete*. RILEM Report 36. -ISBN 2-912143-99-3. 2006. pp. 11-27.
6. Raupach, M., Orlowsky, J., Büttner, T., "Epoxy-impregnated textiles in concrete – load bearing capacity and durability", In: Hegger, J., Brameshuber, W., Will, N. (Edt.), *Proceedings of the 1st International RILEM Conference*, September 6-7, 2006, Aachen, Germany. RILEM Publications S.A.R.L., pp. 77-88.
7. Hegger, J., Kulas, C., Horstmann, M., "Spatial Textile Reinforcement Structures for Ventilated and Sandwich Façade Elements", *Advances in Structural Engineering*, Vol. 15, Issue 4, 2012, pp. 665-675.
8. Büttner, T., Orlowsky, J., Raupach, M., Hojczyk, M., Weichold, O., "Enhancement of the durability of alkali-resistant glass-rovings in concrete", In: Brameshuber, W., *Proceedings of the 2nd International RILEM Conference on Material Science (MatSci)*, September 6-8, 2010, Aachen, Germany. RILEM Publications S.A.R.L., pp. 333-342.
9. Brockmann, T., "Mechanical and fracture mechanical properties of fine grained concrete for textile reinforced composites", PhD-Thesis, Institute of Building Materials Research (ibac), 2006, ISBN 3-86130-631-X.
10. DIN FACHBERICHT 102, "Concrete Bridges", 2009, Beuth Verlag GmbH.
11. Sétra, service d'Études techniques des routes et autoroutes Technical guide Footbridges, Assessment of vibrational behaviour of footbridges under pedestrian loading by Sétra/AFGC working group led by P. Charles and W. Hoorpah, October 2006.
12. Hegger, J., Voss, S., "Investigations on the bearing behaviour and application potential of textile reinforced concrete", *Engineering Structures*, Vol. 30, Issue 7, 2008, pp. 2050-2056.
13. ZTV-ING, „Sammlung Brücken- und Ingenieurbau, Baudurchführung; Zusätzliche Technische Vertragsbedingungen und Richtlinien für Ingenieurbauten (ZTV-ING)", *Verkehrsblatt-Verlag.*
14. Bundesministerium der Justiz, "Ablösungsbeträge-Berechnungsverordnung vom 1. Juli 2010 (BGBl. I pp. 856)".
15. ÖKO-INSTITUT (Institute for applied ecology), "Global Emission Model for Integrated Systems (GEMIS)", version 4.7 (www.gemis.de).